A rheological model for a liquid—gas foam

J. R. Calvert and K. Nezhati*

The flow of a liquid–gas foam may be represented by a modified Bingham plastic model, with the addition of a liquid-rich slip layer caused by bubble migration away from a solid-surface. The model was applied to experimental results for cone and plate rheometer flow and pipe flow. It was found that the consistency and flow behaviour index are to a first approximation independent of expansion ratio and bubble size. The yield stress is dependent on bubble size distribution. The slip layer thickness depends on bubble size distribution and flow geometry, and is the most important parameter in pipe flow. There are changes in foam properties at an expansion ratio around 5 due to the change from gas emulsion to froth configuration.

Keywords: *foam, flow, rheology*

Introduction

Liquid–gas foams have a number of practical applications, for example in fire fighting, foodstuffs and shaving creams. They also occur widely in less desirable situations, for example in many chemical processes. In many of these situations, they are required to flow, and a knowledge of their fluid properties is necessary. These properties may be very different from those of their constituent fluids; the effective viscosity of a water–air foam may be considerably higher than that of either water or air, and the speed of sound lower.

The applications to which the current work is addressed are those where foam flows at an appreciable speed (0.1 to 1 m/s) in pipes of common engineering sizes (10 mm diameter upwards). Examples of such flows are found in fire-fighting equipment, in the pressure relief systems of chemical reactors (particularly under fault conditions), in crude oil pipelines where natural gas may come out of solution to form foams, and in the use of foams for horticultural frost protection. Other similar situations occur in many process industries.

At a fundamental level, the flow properties of a foam can only depend on those of its constituents and on its geometrical configuration. In principle, if complete information were available about the distribution of the bubbles in size, shape and space, it should be possible to deduce the flow properties. In practice, this is not possible due to the difficulties of allowing for interaction between bubbles, migration of bubbles, transients such as liquid film drainage, the unknown effects of shear, and many other such variables. It is therefore necessary to take a more empirical approach.

Various studies have been reported where foam was treated as a homogeneous non-Newtonian fluid. However, this has often been done on a scale which is not directly applicable to engineering problems, eg capillary tube flow[1], or in situations so specific to a particular practical set-up that generalization is not possible, eg Ref 2. Much of the previous work was done before the availability of high computing power, which restricted the modelling to rather simple relationships. No recent work of a general nature on an engineering scale is known to the authors.

The approach used in the current work is to treat the foam as a bulk fluid, and examine its properties during flow on a realistic engineering scale. Various flow models have been fitted to the results, and to try to ensure that the model is adequately flexible two very different geometrical configurations have been used. While it has not proved possible to define completely the geometry of the foams used, care has been taken to ensure that the foam used in different situations was as near as possible identical. All experiments were carried out at or near atmospheric pressure, and all effects of pressure on the foam geometry or properties were ignored.

Definitions of terms

To avoid the confusion of terminology which tends to occur in relation to foams (and multi-phase flows in general), some of the terms specific to foams used in the current work are defined below. Other terms have their normal definitions in fluid mechanics, where appropriate.

Foam: a two-phase material where the continuous phase is liquid and the dispersed phase is gas, where the volume of the gas fraction is not small compared with that of the liquid fraction. This definition covers two rather different structures: at low expansion ratios the structure is of roughly spherical bubbles in a liquid matrix, while at higher expansion ratios polyhedral bubbles are separated by relatively thin liquid films. The two structures are sometimes referred to as gas emulsions and froths, respectively. Close-packed spheres of uniform size will start to interfere at an expansion ratio of 3.7. Where there is a size distribution, higher expansion ratios will be possible. Experimentally, the change appears to occur at expansion ratios around 5.

Expansion ratio: the ratio of the volume of a sample of foam to the volume of its base liquid. This is

* Department of Mechanical Engineering, University of Southampton, Southampton SO9 5NH, UK
Received 20 August 1985 and accepted for publication on 12 February 1986

0142–727X/86/030164–05$3.00

used in preference to void fraction, since relatively high expansion ratios (2 to 10) are used, and void fractions tend to cluster just below 1. The term 'foam quality' which is often found is usually the same as void fraction, but is occasionally defined in terms of mass ratio. Expansion ratio depends on pressure and, since smaller bubbles have higher internal pressures, will vary slightly with average bubble size.

Average bubble size: this may be defined in terms of the mean bubble diameter (probably relevant to the behaviour in shear flows), surface area (relating to surface tension) or volume (which might affect bulk properties such as yield stress). In general the first definition is used, since it is most easily measured and visualized.

Theoretical models

Foams flow in an non-Newtonian manner, and therefore a theoretical model containing a minimum of two parameters is needed. Previous work suggest that yield behaviour is to be expected, so that on of the parameters will be a yield stress. There is no reason to expect linear behaviour is to be expected, so that one of the parameters three parameters would be included. A number of relationships were investigated; the most successful were a generalized Bingham plastic model,

$$\dot{\gamma}=\left(\frac{\tau-\tau_y}{K}\right)^{1/n}$$

and a modified Prandtl–Eyring model,

$$\dot{\gamma}=B\sinh\left(\frac{\tau-\tau_y}{A}\right)$$

In addition to these models of the bulk flow it was assumed that, near to a solid surface, bubble migration would lead to a liquid-rich layer which would have Newtonian characteristics corresponding to the liquid component (at the appropriate temperature). The thickness of this layer, δ, forms a fourth parameter in the theoretical model.

Neither of the above theoretical models is particularly amenable to analytic solution even in very simple geometrical situations. It was therefore decided that a numerical approach would be taken. A computer program was written which could, for any given set of parameters, determine the torque–speed relationship for a cone and plate rheometer. The flow model was contained in its own subroutine, so that any model with up to three parameters and a surface 'slip' layer could be used. This program was then used as a target for the NAG optimization routine E04JBF, to find the best fit between the parameters of the model and experimental results.

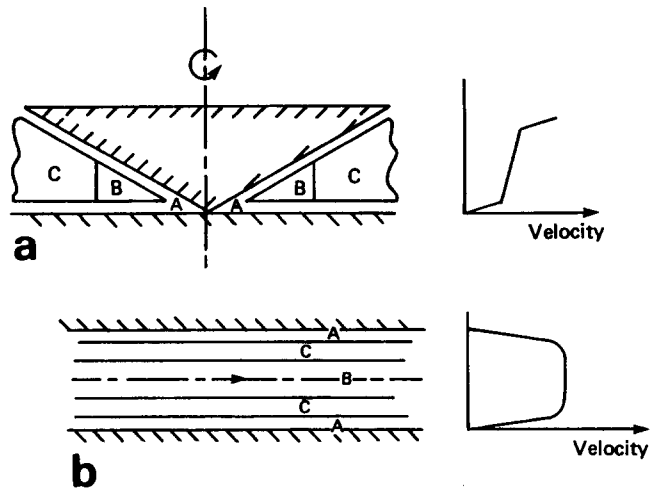

Fig 1 Flow regions (a) in cone and plate rheometer, and (b) in pipe: region A, Newtonian slip layer; region B, unsheared foam; region C, sheared foam. Not to scale

The various regions of flow in the rheometer are shown diagramatically in Fig 1(a). Region A is the sheared Newtonian liquid surface layer, region B is unsheared foam (below yield stress) and region C is sheared foam (above yield stress). At low shear rates region C may be absent, while at high shear rates region B may be absent. The boundaries between the regions were calculated within the program as required.

The flow model parameters thus obtained from the cone and plate results were then used in another program to calculate to flow through straight cylindrical pipes. Since δ was expected to be a function of both foam properties and flow geometry, it was excluded from the input data to this program, and re-calculated by the same optimization routine using experimental data for pipe flow. Fig 1(b) shows the regions of flow for the pipe flow. Again, at low shear rates region C may be absent; region B will always be present.

Experimental details

Foam generation

The foam generator consisted of a mixing chamber fed with pressurized foam liquid solution and air, through separate needle valves. The mixture thus produced then passed through an 'improver' tube containing various baffles and gauzes to the outlet. The liquid and air supplies were fitted with individual flow meters and pressure gauges, and calibration charts were constructed to give the expansion ratio, corrected to atmospheric

Notation

- A Constant in Prandtl–Eyring model
- B Constant in Prandtl–Eyring model
- d Pipe diameter
- K Consistency (modified Bingham plastic model)
- n Flow behaviour index (modified Bingham plastic model)
- Q Foam volumetric flow rate
- R Expansion ratio (defined in text)
- W Water flow rate (arbitrary units)
- $\dot{\gamma}$ Shear rate
- δ Slip layer thickness
- τ Shear stress
- τ_y Yield stress

temperature and pressure, for any supply combination. While this apparatus produced a consistent foam at any one set of settings (so long as the gauzes were kept clean), foam of the same nominal expansion ratio at different flow rates was found to have different properties. This can only be due to different bubble size distributions, and is the subject of further investigation. For the current work, flow rates were carefully controlled to standardized conditions.

The supply pressure to the generator was approximately 5 bar. Liquid flow rates between 9.4 cm^3/s and 21.5 cm^3/s were used; if lower flowrates were required, some flow was bypassed to avoid changing generator conditions.

The generator can produce expansion ratios up to about $R=30$. In the present work, however, R was limited to about 8 for practical reasons.

The foam material used was Kerr 'Hi-Foam' Synthetic Foam Compound (a fire-fighting foam) used in 3% (by volume) aqueous solution. This was chosen for its cost and availability; it was assumed that differences between foam materials would be qualitative only.

Cone and plate rheometer

Because of the relatively large bubble sizes, the rather narrow cone angles (of the order of 2° to 3°) usually used on cone and plate systems are inappropriate. A special instrument was made with an outside diameter of 76.2 mm and a clearance angle of 7°. This instrument was used on a Contraves Rheomat 15 machine, and was calibrated with high viscosity oils. The range of rotational speeds was 5 rev/min to 44 rev/min, giving average shear rates from 4.3 s^{-1} to 38 s^{-1}.

It was found that rheometric measurements had to be made on foam within about 3 min of generation, if problems arising from foam decay were to be avoided.

Pipe flow

Pressure drop measurements were made in straight horizontal lengths of between 1 m and 2 m of polyethylene tubing of 6 different diameters between 12 mm and 32 mm. To avoid throttling of the foam generator output (which will produce unpredictable changes in foam properties[3] the pressure was reduced to near atmospheric pressure by increasing the elevation of the test section relative to the generator. Pressure differences were measured by air–water U-tube manometer. Traps, consisting of sealed Perspex chambers of about 150 mlitre capacity with two tube connections in the top, were provided to prevent foam entering the manometer tubes. The range of shear rates was similar to that for the rheometer measurements: $32Q/\pi d^3$ lay between 4.8 s^{-1} and 110 s^{-1}. The range of average velocity was between about 0.08 m/s and 0.3 m/s.

Results and discussion

Rheometer measurements

Fig 2 shows some experimental data from the rheometer. As can be seen, the curves for different expansion ratios and flow rates have much the same shape, the apparent viscosity falling with increasing shear rate.

Table 1 shows the values obtained when the generalized Bingham plastic model was fitted to the experimental results. Each entry is generated from data covering 8 to 10 different shear rates, between 4.8 s^{-1} and 51 s^{-1}, at the same foam conditions. (Note that in this and subsequent tables, water flow rate is given in arbitrary units, since this is a reference value only, rather than a numerical variable, and is apparatus dependent.) The yield stress averages about 1.5 N/m^2, and never rises above 4 N/m^2. The flow behaviour index n ranges from 0.32 to 0.53. The consistency K ranges from 1.42 to 3.63 (SI units). The correlation coefficients from the optimization process were never below 0.9996.

Very similar results were obtained using the modified Prandtl–Eyring model. However, the correlation coeffiecients were slightly lower, and only the results from the generalized Bingham plastic calculations have been used in further work.

The variations in flow behaviour index and consistency are much less than those of slip layer thickness and yield stress. This suggests that the former properties might, to a first approximation, be independent of flow rate and expansion ratio. Table 2 shows the results re-analyzed with flow behaviour index and consistency set to their average values from Table 1, 0.394 and 2.46, respectively. Very high correlation coefficients were still obtained (none below 0.998). The ranges of yield stress and slip layer thickness were both reduced, although their averages were not much affected.

From Table 2, it is apparent that both yield stress and slip layer thickness are dependent on both expansion ratio and water flow rate. However, the variation with expansion ratio is the more marked. At $R<5$, the maximum yield stress is 1.3 N/m^2, while for $R>5.5$., the minimum is 2.7 N/m^2. Similarly, slip layer thickness falls from around 80 μm at $R=2.5$ to about 25 μm at $R=5$, and then stays roughly constant. These changes at around $R=5$ are thought to be related to the transition from spherical to polyhedral geometry mentioned above. The variation with flow rate shows considerable scatter on the values at a constant expansion ratio, and no real pattern can be discerned. This is not unexpected, since although the bubble size distribution, which is responsible for the variation, will presumably always be the same at the same

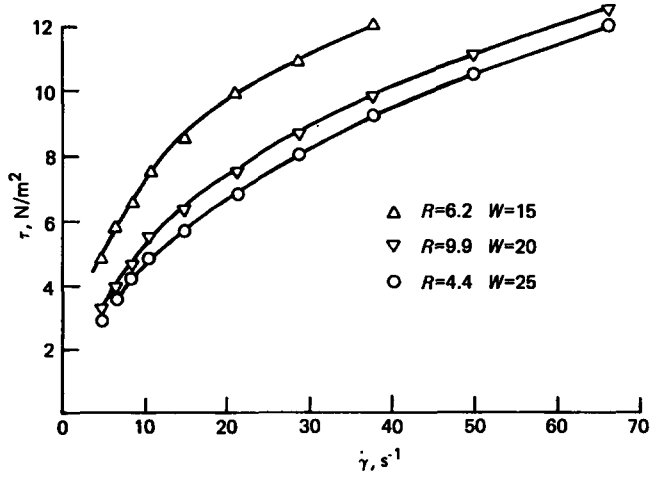

Fig 2 Typical relationships between stress and rate of strain for foam

Table 1 Results from cone and plate rheometer

Expansion ratio	Water flowrate	δ (μm)	τ_y (Nm^{-2})	K (SI)	n	Correlation coefficient
4.1	10	48.7	2.19	1.66	0.473	0.9996
3.0	15	65.4	1.71	2.38	0.378	0.9998
2.6	20	55.4	1.63	2.24	0.395	0.9998
2.4	25	70.7	1.97	1.95	0.419	0.9998
4.7	10	33.9	1.88	2.38	0.386	0.9998
3.7	15	39.3	2.25	1.99	0.422	0.9999
3.1	20	53.8	0.02	3.60	0.319	1.0000
2.9	25	85.6	1.33	1.98	0.438	0.9998
5.8	10	20.4	4.03	1.42	0.530	0.9999
4.2	15	23.0	0.24	2.67	0.378	1.0000
3.5	20	53.6	1.56	2.41	0.384	0.9999
3.0	25	38.9	0.30	3.15	0.347	0.9999
7.1	10	15.9	0.42	3.51	0.345	0.9999
5.2	15	30.6	2.38	2.32	0.389	0.9999
4.2	20	48.8	1.60	2.55	0.361	0.9997
3.6	25	38.9	2.04	2.45	0.375	0.9998
6.1	15	21.9	1.51	3.63	0.321	0.9999
5.0	20	33.8	0.74	2.70	0.375	1.0000
4.2	25	38.6	1.54	1.75	0.459	0.9999

Table 2 Results from cone and plate rheometer using averaged values of K and n

Expansion ratio	Water flowrate	δ (μm)	τ_y (Nm^{-2})	Correlation coefficient
4.1	10	51.0	1.21	0.9994
3.0	15	63.5	1.02	0.9988
2.6	20	49.1	0.60	0.9993
2.4	25	74.3	0.99	0.9980
4.7	10	26.6	0.98	0.9994
3.7	15	34.7	1.04	0.9996
3.1	20	53.7	1.32	0.9998
2.9	25	89.8	0.98	0.9997
5.8	10	22.9	3.12	0.9989
4.2	15	22.7	0.48	0.9999
3.5	20	49.4	0.92	0.9996
3.0	25	40.0	1.21	0.9999
7.1	10	22.9	2.71	0.9997
5.2	15	25.8	1.54	0.9994
4.2	20	36.8	0.41	0.9985
3.6	25	32.5	1.17	0.9990
6.1	15	22.6	3.02	0.9998
5.0	20	33.1	0.95	0.9999
4.2	25	35.0	0.34	0.9998

K=0.246, n=0.394

Table 3 Results from pipe flow experiments

Expansion ratio	Water flowrate	δ (μm)
4.2	10	15.5
3.2	15	22.6
2.7	20	26.6
2.4	25	35.2
5.2	10	17.5
3.8	15	24.8
3.2	20	32.9
2.8	25	39.2
6.0	10	12.9
4.4	15	11.5
3.7	20	20.8
3.1	25	30.6
7.4	10	7.75
5.4	15	15.1
4.4	20	19.5
3.7	25	29.1
6.4	15	13.6
5.2	20	12.0
4.4	25	20.7

τ_y, K and n have the appropriate values from the cone and plate results

flow rate and expansion ratio, it is not necessarily linked in any simple manner to the flow rate.

Pipe flow measurements

The values of yield stress, consistency and flow behaviour index obtained from the cone and plate measurements were used to analyse the pipe flow results. For each combination of expansion ratio and generator flow rate, the optimum value of slip layer thickness was calculated for six different pipe diameters and three different pipe lengths. There was reasonable correlation for slip layer thickness between results for different diameters. Typical values were about half those for the cone and plate results, ranging from 7.8 μm to 39 μm (Table 3). Again, there is evidence of a change at around $R=5$, with values levelling off at about 13 μm.

Calculated velocity profiles show plug flow (below yield stress) over about 65% of the diameter, with a slip velocity of 75–95% of mean velocity. The flow rate is thus primarily controlled by the slip, and only secondarily by the shear; if the slip layer thickness can be estimated, the flow rate could be predicted with fair accuracy from a knowledge of the wall shear stress (pressure gradient) and

the viscous properties of the base liquid only. Since the slip layer thickness must be related to the bubble size, knowledge of the bubble size distribution is clearly vital. Preliminary measurements (which are continuing) show that the slip layer thickness is well below the average bubble size, and compares with the diameters of the smallest bubbles present in any quantity (about the 10th percentile on diameter).

Conclusions

Rheometer experiments showed that the flow of fire-fighting foam can be modelled by a modifed Bingham Plastic system, with a liquid-rich slip layer at solid surfaces. The results from this model can be used to describe the flow of the same foam through pipes.

The consistency and flow behaviour index were found to be to a large extent independent of the flow rate and expansion ratio for the particular foams tested (although they could well be different for foams produced by other methods). The yield stress varied much more strongly with both flow rate and expansion ratio. This variation, it was concluded, must arise through differences in bubble size distribution.

The thickness of the slip layer depends on the expansion ratio and flow rate (bubble size distribution) of the foam, and also on the flow conditions. Further work is in progress on the relationship between slip layer thickness and bubble size.

The slip layer thickness dominates the pipe flow behaviour over this range of shear rates.

There is a change in foam properties at expansion ratios around 5 which is probably related to the change from a spherical to a polyhedral geometry.

Acknowledgements

The work was carried out in the Mechanical Engineering Department, University of Southampton, under a grant from the Science and Engineering Research Council. The foam generator was lent by the Department of the Environment, Fire Research Station, who also supplied foam concentrate.

References

1. **David, A.** *The Rheology of Foam; PhD Thesis, Stanford University Department of Petroleum Engineering, 1968*
2. **Grove, C. S., Wise, G. E. and Marsh, J. B.** Viscosity of fire-fighting foam. *Ind. and Eng. Chem., 1951,* **43**, *1120–1122*
3. **Jones, S.** *The Effect of Flow through Valves on Fire-fighting Foam Characteristics; Project Report, Southampton University Department of Mechanical Engineering, 1984 (unpublished)*

CALENDAR

ASME Winter Annual Meeting: International Symposium on Pressure and Temperature Measurement	30 November–5 December 1986 San Francisco, CA, USA	Dr J. H. Kim, Electric Power Research Institute, 3412 Hillview Avenue, PO Box 10412, Palo Alto, CA 94303, USA
Modern Industrial Liquid Mixing Technology	1–4 December 1986 The Hague, The Netherlands	The Center for Professional Advancement, Palestrinastraat 1, 1071 LC Amsterdam, The Netherlands
Australian Fluid Mechanics Conference	8–12 December 1986 Auckland, New Zealand	AFMC Conference Committee, c/o Dr P. S. Jackson, Dept of Mechanical Engineering, Auckland University, Private Bag, Auckland, New Zealand
10th BPMA Technical Conference on Pumps	24–26 March 1987 Cambridge, UK	BHRA Fluid Engineering Centre, Cranfield, Bedford MK43 0AJ, UK
Large Scale Applications of Heat Pumps	25–27 March 1987 Oxford, UK	BHRA Fluid Engineering Centre, Cranfield, Bedford MK43 0AJ, UK
11th International Conference on Fluid Sealing	8–10 April 1987 Cannes, France	BHRA Fluid Engineering Centre, Cranfield, Bedford MK43 0AJ, UK
International Meeting on Heat Transfer	13–17 April 1987 Lyon, France	Professor, J. F. Sacadura, INSA de Lyon, LMFT Bat. 302-20 Ave. Albert Einstein, 69621 Villeurbanne Cedex, France
International Conference on Flow Induced Vibrations	12–14 May 1987 Bowness-on-Windermere, UK	BHRA Fluid Engineering Centre, Cranfield, Bedford MK43 0AJ, UK
3rd International Conference on Multi-Phase Flow	18–20 May 1987 The Hague, The Netherlands	BHRA Fluid Engineering Centre, Cranfield, Bedford MK43 0AJ, UK
6th Turbulent Shear Flow Symposium	7–9 September 1987 Toulouse, France	Professor F. W. Schmidt, Secretary, Dept of Mechanical Engineering, The Pennsylvania State Univ., University Park, PA 16802, USA
Second International Conference on Laser Anemometry	21–23 September 1987 Glasgow, Scotland, UK	Dr S. M. Fraser, LDA Conference, Mechanical and Offshore Engineering, University of Strathclyde, Glasgow G1 1XJ, UK
International Symposium on Natural Circulation	15–20 November 1987 New York, NY, USA	Dr J. H. Kim, Electric Power Research Institute, PO Box 10412, Palo Alto, California 94303, USA